High Bandwidth Measurements of Auroral Langmuir Waves with Multiple Antennas

Chrystal Moser[1] James LaBelle[1] Iver H. Cairns[2]

[1]Department of Physics and Astronomy, Dartmouth College, Hanover, NH, [2]School of Physics, University of Sydney, Sydney, AU

Abstract

The High-Bandwidth Auroral Rocket (HIBAR) was launched from Poker Flat, Alaska on January 28, 2003 at 07:50 UT towards an apogee of 382 km in the night-side aurora. The flight was unique in having three high-frequency (HF) receivers using multiple antennas parallel and perpendicular to the ambient magnetic field, as well as very low frequency (VLF) receivers using antennas perpendicular to the magnetic field. These receivers observed five short-lived Langmuir wave bursts lasting from 0.1-0.2 s, consisting of a thin plasma line with frequencies in the range of 2470--2610 kHz that had an associated diffuse feature occurring 5--10 kHz above the plasma line. Both of these waves occurred slightly above the local plasma frequency with amplitudes between 1-100 μV/m. The ratio of the parallel to perpendicular components of the plasma line and diffuse feature were used to determine the angle of propagation of these waves with respect to the background magnetic field. These angles were compared to the theoretical Z-infinity angle that these waves would resonate at, and found to be comparable. The VLF receiver detected auroral hiss at frequencies between 5-10 kHz throughout the flight from 100-560 s, a frequency matching the difference between the plasma line and the diffuse feature. A dispersion solver and associated frequency- and wavevector-matching conditions were employed to determine if the diffuse features could be generated by a nonlinear wave-wave interaction of the plasma line with the lower frequency auroral hiss waves. The results show that this interpretation is plausible.

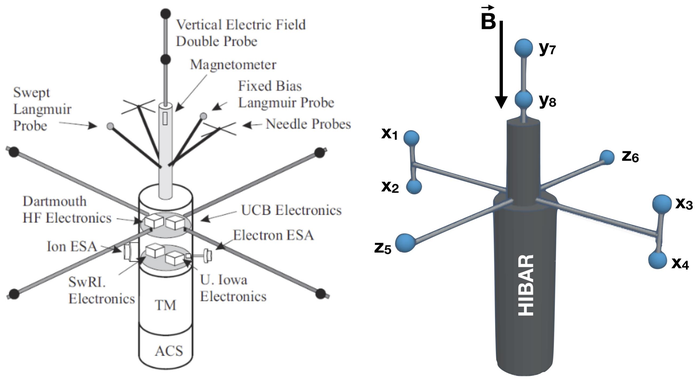

Figure 1. Diagram of the TRICE-2 (left) and HIBAR (right) rockets. The TRICE-2 diagram shows all the instruments from the contributing institute. The HIBAR diagram shows the antenna orientation with respect to the background magnetic field.

Conclusion

- TRICE-2
  - Banded UH waves, with spacings of ~5 kHz, occur coincident with distinct LH wave at a frequency of ~5 kHzs
  - Spectral analysis of the UH frequency spacing versus the LH peaks frequency shows a close correlation
  - Frequency and wavevector matching conditions were used with WHAMP and the waves were found to occur in areas of growth
- HIBAR
  - Short bursts (0.1-0.2 s) of plasma waves close to the local plasma frequency with an associated diffuse region of waves 5-15 kHz above observed by both the parallel and perpendicular antenna
  - VLF Spectrogram shows broadband whistler mode waves from 5-15 kHz
  - Ratios of parallel to perpendicular electric fields show the diffuse wave is more perpendicular than the plasma wave, in line with accepted plasma theory
  - Frequency and wavevector analysis using WHAMP suggests there is a third VLF wave that could plausibly interact with the plasma wave to produce the diffuse feature.

References

1. Colpitts, C. and LaBelle, J.: Mode identification of whistler mode, Z-mode, and Langmuir/Upper Hybrid mode waves observed in an auroral sounding rocket experiment, Journal of Geophysical Research: Space Physics, 113, 2008.
2. Dombrowski, M., LaBelle, J., Rowland, D., Pfaff, R., and Kletzing, C.: Interpretation of vector electric field measurements of bursty Lang-3muir waves in the cusp, Journal of Geophysical Research: Space Physics, 117, 2012..
3. McFadden, J., Carlson, C., and Boehm, M.: High-frequency waves generated by auroral electrons, Journal of Geophysical Research: Space Physics, 91, 12 079–12 088, 1986
4. Moser, C., LaBelle, J., Roglans, R., Bonnell, J., Cairns, I., Feltman, C., Kletzing, C., Bounds, S., Sawyer, R., and Fuselier, S.: Modulated Upper-Hybrid Waves Coincident with Lower-Hybrid Waves in the Cusp, Journal of Geophysical Research: Space Physics, 2021

TRICE-2 Upper-Hybrid Waves

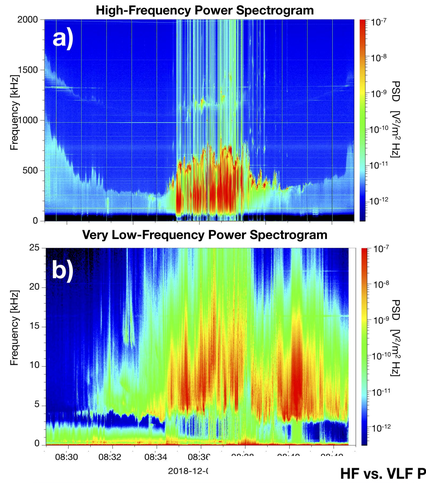

Figure 2. Spectrograms from 08:29-08:43 UTC during TRICE-2 High-Flyer's passage through the cusp. (a) HF power from 100-2000 kHz, showing and increase in the intensity and frequency of Langmuir waves between 08:34:30-08:39:20 UTC (frequencies 400-800 kHz) corresponding to the increase in density in the cusp. (b) VLF wave power from 0-25 kHz with intense broadband whistler waves occurring above the LH cutoff at ~5 kHz within and poleward of the cusp. The power spectral density ranges from 1E-13 to 1E-6 for both the UH and LH spectrograms

Figure 3. Expanded views of the HF and VLF Spectrograms, showing the banded structure in the UH waves in the HF spectrograms and the distinct LH waves that occur below the broadband whistler mode waves in the VLF spectrograms at ~5 kHz. The white lines in panels (a) and (c) is the UH frequency calculated using the plasma frequency cutoff and the magnetometer data, at an altitude of ~1000 km.

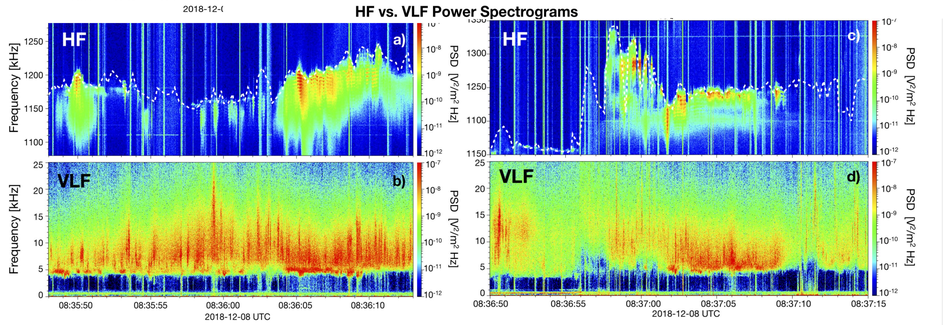

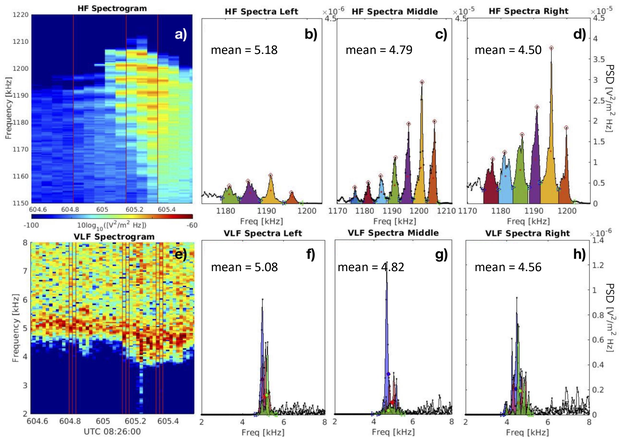

Figure 4. (a) Expanded HF Spectrogram of banded structures for the time interval 08:36:04.6-08:36:05.6 UTC for frequencies 1150-1220 kHz. (e) Same time interval for the expanded VLF spectrogram from 2-8 kHz, showing peaks at the LH frequency. (b-d) Three selected spectra from the HF data showing the variation in peak spacings. (f-h) Nine selected spectra, three for each HF spectra, showing the peak variations over time. The HF spacing changes with the changes in frequency of the VLF peak.

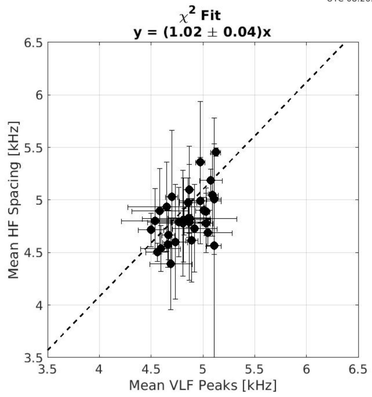

Figure 5. Plot of the average HF bands frequency spacings versus the average LH peak frequencies , with their respective standard deviations plotted as bars on the points. The linear fit (black dashed) is plotted and is baded on the variance in both x and y, with a slope of .02 ± 0.04 [kHz/kHz].

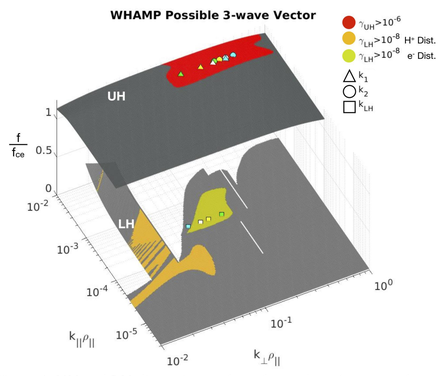

Figure 6. UH and LH dispersion surfaces focused on the areas of growth, where the plateaus roughly equal the UH and LH frequencies. On the UH surface, the four differently colored triangle points represent four possible initial UH wavevectors. The Four circles represent the corresponding second UH wave, matching in color. The LH surface shows the calculated LH wavevectors from the frequency and wavevector matching condition.

HIBAR Langmuir Waves

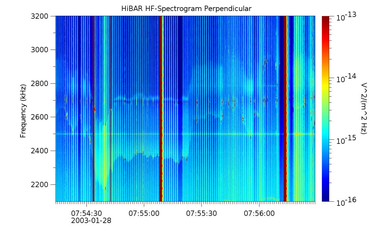

Figure 7. Spectrograms of HF and VLF from HIBAR from 07:54:14-07:56:29 UT. (a) HF spectrogram from the perpendicular antenna showing the plasma frequency cutoff as a lower bound and the UH frequency as an upper cutoff, (b) HF spectrogram from the parallel andteenna showing the plasma frequecy as a lower cutoff equal to the perepndicualr antenna. (c) VLF spectrogram showing the LH frequency cutoff as a lower bound with broadband whistler spanning from 5-25 kHz.

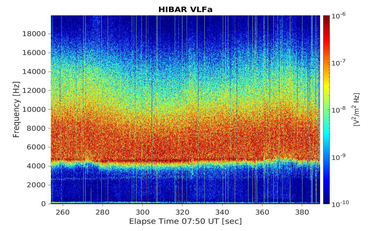

Figure 8. 2000-3200 kHz spectrograms of perepndicular (upperpanels a & c) and parallel (lower panels b & d) HF electric field for two time intervals during the HIBAR flight: 07:54:18-07:54:33 UT and 07:55:49-07:36:04 UT , showing the plasma frequency cutoff as a lower bound. Red circles indicate five Langmuir waves bursts used for detailed study.

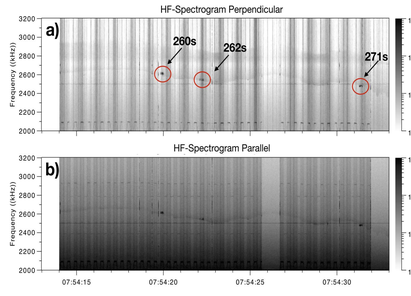

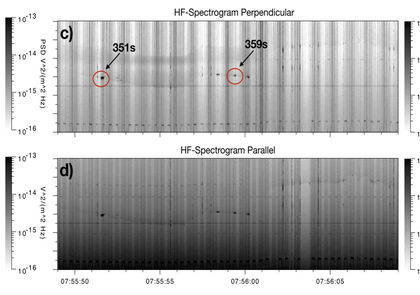

Figure 9. Enhanced plots of the five Langmuir bursts indicated in Figure 2, presented in time order, each comprised of a narrow band plasma line and a broadband diffuse feature with ~5–15 kHz higher frequency. The top panels in each plot are from the perpendicular antenna, the middle panels are from the parallel antenna, and the bottom panels are the parallel to perpendicular ratios of the amplitudes of the plasma peaks (red) and the diffuse feature (blue).

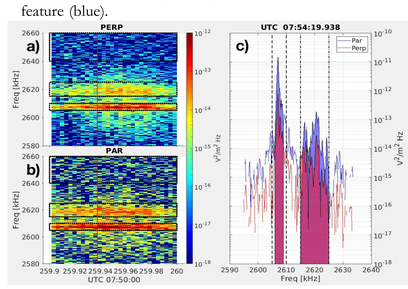

Figure 10. (a) Perpendicular and (b) parallel spectrograms for the Langmuir bursts labeled 260s in Figure 2 and shown in Figure 4a. Black boxes indicate the frequency-time ranges used to define the plasma line, diffuse feature, and background level. (c) Selected spectrum with background noise subtracted, occurring at the time highlighted as a red vertical line in panels (a) and (b), showing the power spectral density of the parallel waves (blue) versus the perpendicular waves (red).

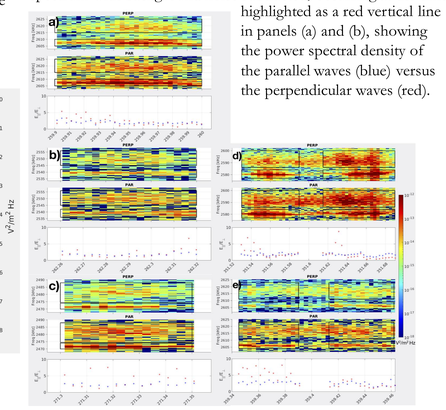

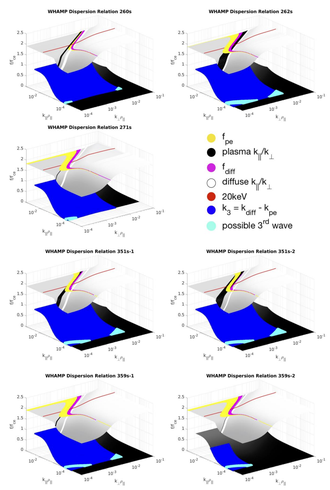

Figure 11. WHAMP dispersion surfaces for Langmuir bursts labeled in Figures 2–4, with k || /k ⊥ ratios inferred from the maximum E || /E ⊥ in Table 1 plotted as black for the plasma line and white for the diffuse feature. The yellow and pink areas indicate where the surface matches the frequency of the plasma line and diffuse feature, respectively. Where these intersect defines the range of possible k-vectors for each wave. Assuming wave-wave interaction, kinematic equations imply a range of k-vectors for the possible third wave plotted in dark blue on the whistler/LH surface, and the matching frequency of the third wave plotted in light blue.

[1]Department of Physics and Astronomy, Dartmouth College, Hanover, NH
[2]School of Physics, University of Sydney, Sydney, AU

Aknowledgements

Thanks to the team at Wallops Flight Facility and NASA for supporting the HIBAR payload and launch, as well as engineer Hank Harjes and NASA engineer Bill Payne for instrumentation support. Thanks to R. Roglans, J. Bonnell, C. Feltman, C. Kletzing, S. Bounds, R. Sawyer, S. Fuselier for contributions and support for the TRICE-2 work. Authors also thank S. Marilia, C. Feltmann, and S. Bounds for discussions and support with the HIBAR research. Research at Dartmouth College was supported by NASA grant NNX17AF92G.